Supplemental Information

Proper synaptic vesicle formation and neuronal network activity critically rely on syndapin I

Dennis Koch *et al*

Legends of Supplementary Figures

Supplementary Figure S1 Quantitative comparison of expression levels of selected proteins analyzed in brain homogenates of WT and syndapin I KO mice.

For quantification of a particular protein in WT and syndapin I mice (n=5 for each genotype), the signal intensities were normalized to the actin signal on the same membrane. Mean signal in WT was set to 100%. No statistically significant changes were evident using Mann-Whitney-U-test. Data represent mean ± sem in percent. Typical results of Western blot analyses are shown in Fig. 1J.

Supplementary Figure S2 Syndapin I KO mice show an increased volume of the hippocampus.

(**A,B**) Manganese-enhanced magnetic resonance imaging of WT and syndapin I KO mice (**A**) and quantitative volumimetric analyses (**B**) showed an increase of hippocampal volume by 7% in syndapin I KO mice (n=9 animals for +/+, n=8 animals for -/-; Mann-Whitney-U-test; *$p<0.05$). Data represent mean±sem. Bo, bulbus olfactoris; Co, cortex; Pu, putamen; Th, thalamus; Hc, hippocampus; Ce, cerebellum. Bar, 5 mm.

Supplementary Figure S3 Unchanged F-/G-actin ratio in syndapin I KO mice.

(**A,B**) Quantification of F-/G-actin ratio in the hippocampus. (**A**) Confocal laser-scanning micrographs of the hippocampus stained for G-actin using Alexa Fluor®488-DNaseI (green in merge) and for F-actin using Alexa Fluor®568-phalloidin (red in merge). Nuclei were stained with DAPI (blue in merge). For each slice, actin levels were quantified on 5 ROIs (examples in white) located in the inner molecular layer of the dentate gyrus. Bar, 100 µm. (**B**) Quantifications of the F-/G-actin ratio did not reveal any changes upon syndapin I KO (n=17 (+/+) and 15 (-/-) from 4 adult animals). (**C,D**) Biochemical quantification of F-/G-actin in synaptosomes. Western blot analysis of synaptosomal G- and F-actin is shown in (**C**). Quantification of F-/G-actin ratio levels did not point to significant changes between WT and syndapin I KO mice (5 preparations from 3 adult animals of each genotype) (**D**).

Supplementary Fig. S4 Immunohistochemistry of syndapin I in the retina.

Confocal laser-scanning micrographs of photoreceptor ribbon synapses (**A-C**) double labeled for the presynaptic marker RIBEYE (**A**) and syndapin I (**B**) and merges thereof (**C**). Syndapin I is widely expressed in the retina with a peak of expression in the outer plexiform layer (OPL) (**B**). A significant proportion of syndapin I localizes to rod photoreceptors as it overlaps with RIBEYE (**C**). Scale bar, 20 µm. OS, outer segments. ONL, outer nuclear layer. INL, inner nuclear layer. IPL, inner plexiform layer.

Supplementary Figure S5 Immunocytochemistry of dynamins in primary hippocampal cultures at 21 DIV from WT and syndapin I KO mice.

(**A-J**) Anti-dynamin I immunosignals partially colocalize with the pre- and postsynaptic marker proteins bassoon and ProSAP2, respectively (**A,F**). No obvious changes in localization or

fluorescence intensity of dynamin I (**E**,**J**) upon syndapin I deficiency were detectable in neurites at the light microscopical level as seen in the magnifications (**B-E,G-J**).

(**K-T**) Immunolocalization of dynamin II and the pre- and postsynaptic marker proteins bassoon and ProSAP2 (**K,P**). The analysis did not reveal differences in localization or fluorescence intensity of dynamin II (**O**,**T**) between the genotypes as seen in the magnifications (**L-O,Q-T**).

(**U-Λ)** Anti-dynamin III immunosignals intensively colocalize with the pre- and postsynaptic marker proteins bassoon and ProSAP2 (**U**,**Z**). There was no evidence for changes in dynamin III (**Y**,**Λ**) localization and/or protein level upon syndapin I deficiency as seen in the magnifications (**V-Y, Γ-Λ**). Scale bars, 20 µm.

Supplementary Figure S6 Syndapin I participates in dynamin recruitment to the plasma membrane during SV formation.

Scenario how syndapin I participates in dynamin recruitment during SV generation. Generation of SVs in WT animals is supported by syndapin I binding to the curved membranes generated during vesicle formation and by the ability of syndapin I to recruit dynamin to these sites at the plasma membrane. Together, this ensures proper SV formation. In contrast, in syndapin I KO animals, the lack of syndapin I leads to delayed and/or inefficient dynamin recruitment. A prolonged maturation of the forming vesicle leads to enlarged SVs, as observed in syndapin I KO synapses of different origin.

Supplementary Figure S7 Syndapin I binds to the dynamin III PRD directly.

Coprecipitation assay with purified fusion proteins proved a direct interaction between syndapin I and the PRD of dynamin III. Equal amounts (30 µg) of GST and GST-dynamin III PRD were immobilized on glutathione-coupled beads and subsequently incubated with 30 µg of His-thioredoxin or His-thioredoxin-tagged syndapin I fusion proteins. Syndapin I was specifically

precipitated by beads coated with GST-dynamin III-PRD. The order of samples on the gels was modified, as indicated by white lines. PD, pull down.

Supplementary Figure S8 SDS-PAGE/Coomassie analysis of starting material for liposome binding assays.

WT and syndapin I KO cytosol (n=2 for +/+ and -/-) used in the liposome binding assays (please see Fig. 6G,H) were separated via SDS-PAGE. Subsequent protein staining using Coomassie Brilliant Blue showed that protein levels are equal in WT and syndapin I KO cytosol (15 µg protein loaded).

Supplementary Figure S9 Anti-syndapin I immunohistochemistry of hippocampal areas.

(**A,B**) Staining of syndapin I in the hippocampus of WT (**A**) and syndapin I KO (**B**) mice revealed a specific pattern throughout the hippocampus. Dentate gyrus (DG) and CA1, CA2, CA3 regions of the hippocampus are marked.

(**C-H**) Syndapin I is widely expressed in the brain and is also present in inhibitory neurons, as identified by colocalization with parvalbumin (arrows). Immunstainings of the CA2 region (**C-E**) and of the dentate gyrus (**F-H**) are shown. Bars, 250 µm (**A,B**), 50 µm (**C-E**) and 100 µm (**F-H**).

Supplementary Figure S10 Syndapin I KO mice show a slightly reduced synaptic fatigue at 20 Hz but not at lower and higher stimulation frequencies.

(**A-E**) Synaptic fatigue monitored at frequencies of 2 (**A**), 5 (**B**), 20 Hz (**C**), 50 Hz (**D**) and 100 Hz (**E**), respectively, in the presence of 100 µM picrotoxin. Exclusively at 20 Hz, syndapin I KO mice displayed a significantly weaker depression (**C**). Data represent mean ± sem. N-numbers represent examined hippocampal slices (derived from 8 WT and 9 KO animals). 2-Way repeated measures ANOVA was applied for **A-E**. *$p<0.05$.

Supplementary Figure S11 Syndapin I protein levels increase dramatically during brain development.

Equal amounts (50 µg) of brain homogenates of different developmental stages (n=2 each) were analyzed for the presence of syndapin I (**A**) and tubulin (**B**). For quantification of syndapin I protein levels, defined amounts of purified GST-syndapin I (0.5-40 ng) on the same Western blot membrane served as standards (**A**). Quantification of syndapin I in brain homogenate (50 µg total brain protein) revealed a strong increase from 1.4 ng (0.028 mg/g total brain protein) (E18), 2.5 ng (0.050 mg/g total brain protein) (P0), 3.4 ng (0.068 mg/g total brain protein) (P4) to 38.2 ng (0.76 mg/g total brain protein) [adult (P84)] during development (**C**).

Supplementary Movie 1. Syndapin I KO mice suffer from generalized seizures with tonic-clonic convulsions.

Movie 1 shows a typical example of spontaneous seizures of a syndapin I KO mouse upon transfer into a new cage. The syndapin I KO mouse stops moving and undergoes partial seizures culminating in tonic-clonic convulsions. Afterwards, the mouse sits up again very quietly. After this pause it resumes to move around normally.

Supplemental Experimental Procedures

Animals

The mice were kept under constant laboratory conditions (12 h light, 12 h dark; 100 lux at cage bottom). All animal experiments were performed in compliance with the guidelines for the welfare of experimental animals issued by the Federal Government of Germany and the National Institutes of Health.

Primer Information

Primer No.	Primer Sequence	purpose
BQ108	AAGCGGACGGTGAAGCGCATCGA	Screening for suitable BAC clone
BQ109	TCGATGAGCTGGCGCCAGCGCTT	Screening for suitable BAC clone
BQ115	TGAACAGCAGAAGAAACTTG	Southern Blot probe
BQ364	GCCAATAGCAGCTTTGCTCCTT	PCR for right arm
BQ368	GCATTACTCACGCCCAGTGTCCTTTC	PCR for left arm
BQ371	CAAACTGCTGGCACTGCTCAAACAC	Southern Blot probe/PCR for right arm
BQ443	GCGAAGGAGCAAAGCTGCTATTGGC	PCR for left arm
BQ497	AAGGGAGTCTGGATGCAAGG	Genotyping of WT allele
BQ502	AGAGATGTTGAGATGTGTAC	Genotyping of WT allele
BQ498	ATCTGAGGAGACCCATTCAG	Genotyping of KO allele
BQ536	CGGTAGAATTGACGAAGTTCC	Genotyping of KO allele
BQ537	ATTTGCCTGCATTACCGGTC	Genotyping of *Cre* allele
BQ538	ATCAACGTTTTCTTTTCGGA	Genotyping of *Cre* allele
BQ976	GACGAATTCAACACGGTCACTGTG	Amplification of dynamin IIIbaa PRD
BQ977	GTCGTCGACTTAGTCTAACAGTGA	Amplification of dynamin IIIbaa PRD

Antibodies

Primary antibodies used in this study were purchased from ABR (anti-dynamin I), Assay Designs (anti-bassoon), BD Biosciences [anti-amphiphysin I, anti-AP2 (µ2), anti-pan-dynamin, anti-PSD-95, anti-RIBEYE, anti-Sos, anti-synaptojanin I], Sigma (anti-β-actin, anti-MAP2, anti-β-tubulin), Synaptic Systems (anti-AP180, anti-gephyrin, anti-parvalbumin, anti-synaptophysin I, anti-synapsin Ia/b ; anti-clathrin light chain), Upstate (anti-cortactin) and Zymed (anti-endophilin I). Further antibodies were kind gifts from M. McNiven (anti-dynamin II and anti-dynamin III) and T. M. Böckers (anti-ProSAP2) and were generated in the course of our studies [anti-Abp1 (Qualmann *et al*, 2004), anti-EHD (Braun *et al*, 2005), anti-GST (Qualmann *et al*, 1999, this study), anti-His (this study), anti-N-WASP (Kessels and Qualmann, 2002), anti-syndapin I (Qualmann *et al*, 1999), anti-syndapin II (Qualmann *et al*, 2000), anti-syndapin III (this study)], respectively.

Secondary antibodies for Western blot analyses were from Jackson immunoresearch (goat-anti-rabbit-POX), Dianova (goat-anti-guinea pig-POX), Invitrogen (goat-anti-rabbit-Alexa Fluor®680, goat-anti-mouse-Alexa Fluor®680), Pierce (goat-anti-rabbit-DyLight800, goat-anti-mouse DyLight800) and LI-COR (donkey-anti-guinea pig-IRDye680). Secondary antibodies for immunocytochemistry were from Invitrogen (Alexa Fluor®488, Alexa Fluor®568, Alexa Fluor®647).

Coprecipitation of recombinant syndapin I and dynamin III PRD

GST-dynamin IIIbaa PRD was cloned into pGEX5x1 (Amersham) by PCR. GST-dynamin IIIbaa PRD or GST alone (30 µg each) coupled to GST high affinity resin (Genscript) were incubated with 30 µg of His-thioredoxin-tagged syndapin I or His-thioredoxin alone in HCB buffer containing 250 mM NaCl, 1% TritonX-100, 1 mM DTT, Complete®EDTA-free and 0.1 mg/ml BSA. After extensive washing, bound proteins were subjected to Western blot analysis.

Supplemental Reference

Qualmann B, Boeckers TM, Jeromin M, Gundelfinger ED, Kessels MM (2004) Linkage of the actin cytoskeleton to the postsynaptic density via direct interactions of Abp1 with the ProSAP/Shank family. *J Neurosci* **10**: 2481-2495

Supplementary Figure 1

protein	+/+ n=5 mean ± sem	-/- n=5 mean ± sem
syndapin I	100 ± 14	0 ± 0
syndapin II	100 ± 13	92 ± 7
syndapin III	100 ± 15	98 ± 15
amphiphysin I	100 ± 5	102 ± 7
endophilin I	100 ± 12	96 ± 13
Abp1	100 ± 20	95 ± 16
cortactin	100 ± 11	98 ± 13
Sos	100 ± 6	92 ± 5
EHD	100 ± 19	93 ± 16
synapsin Ia/b	100 ± 8	103 ± 8
N-WASP	100 ± 9	91 ± 15
dynamin I	100 ± 4	101 ± 3
dynamin II	100 ± 10	91 ± 10
dynamin III	100 ± 6	100 ± 9
synaptojanin I	100 ± 14	100 ± 18
clathrin HC	100 ± 7	89 ± 7
AP2	100 ± 10	113 ± 13
AP180	100 ± 5	103 ± 11
synaptophysin I	100 ± 6	91 ± 11
PSD95	100 ± 10	91 ± 11
gephyrin	100 ± 3	111 ± 8
tubulin	100 ± 1	101 ± 2
actin	100 ± 4	102 ± 2

Supplementary Figure 2

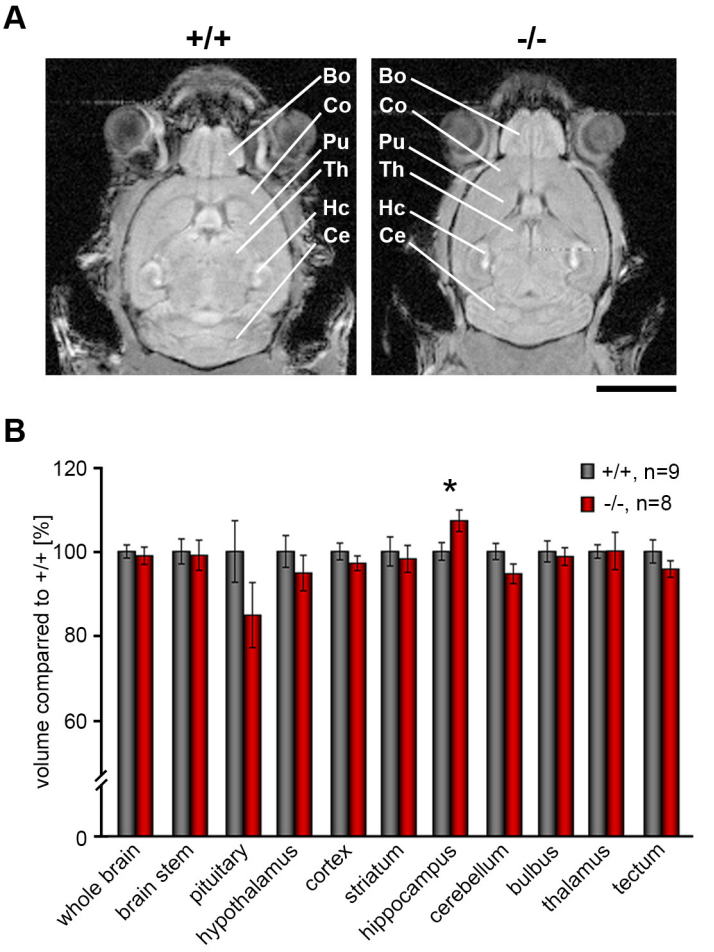

Supplementary Figure 3

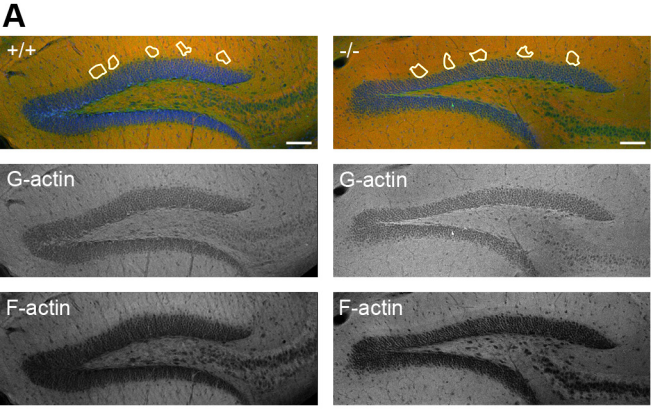

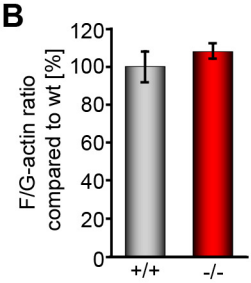

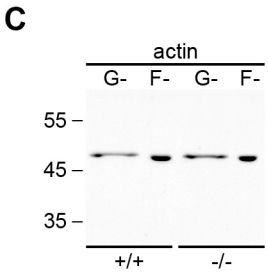

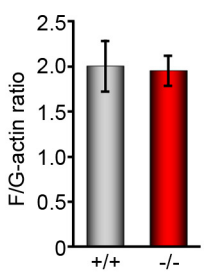

Supplementary Figure 4

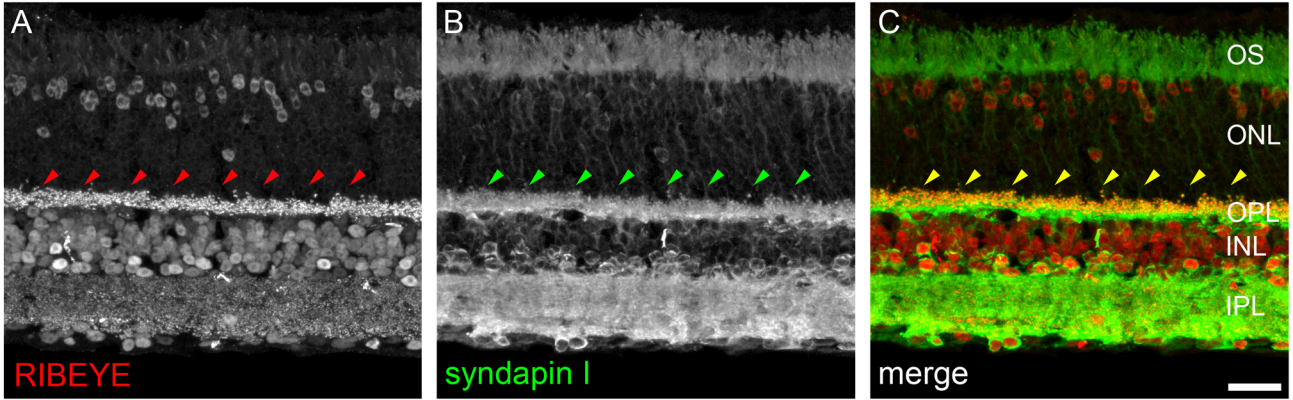

Supplementary Figure 5

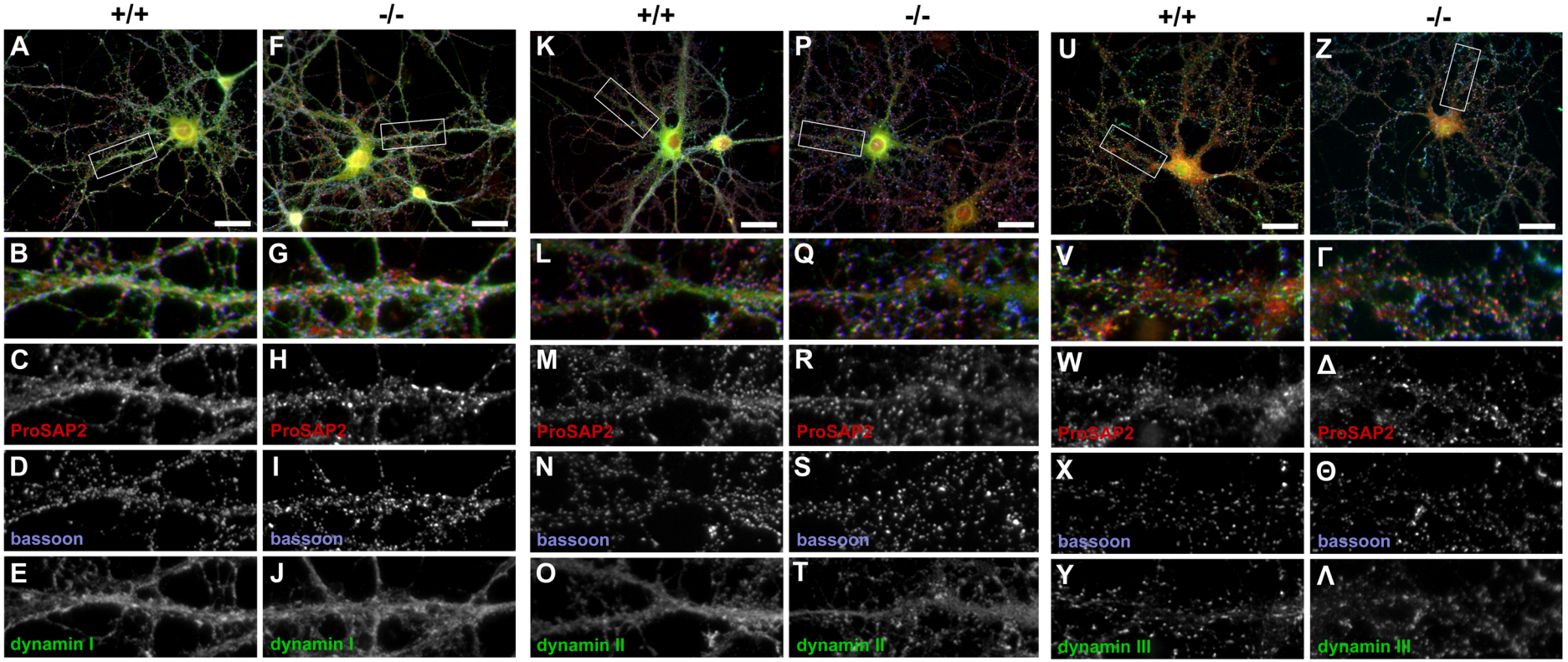

Supplementary Figure 6

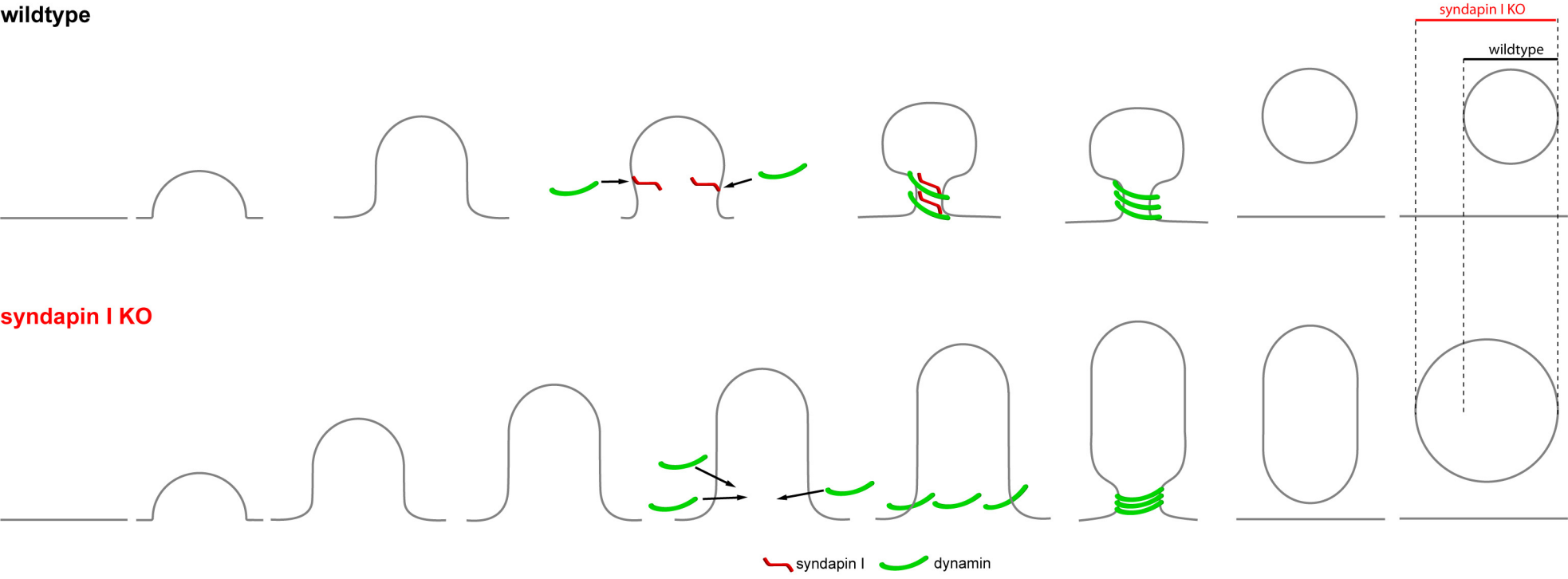

Supplementary Figure 7

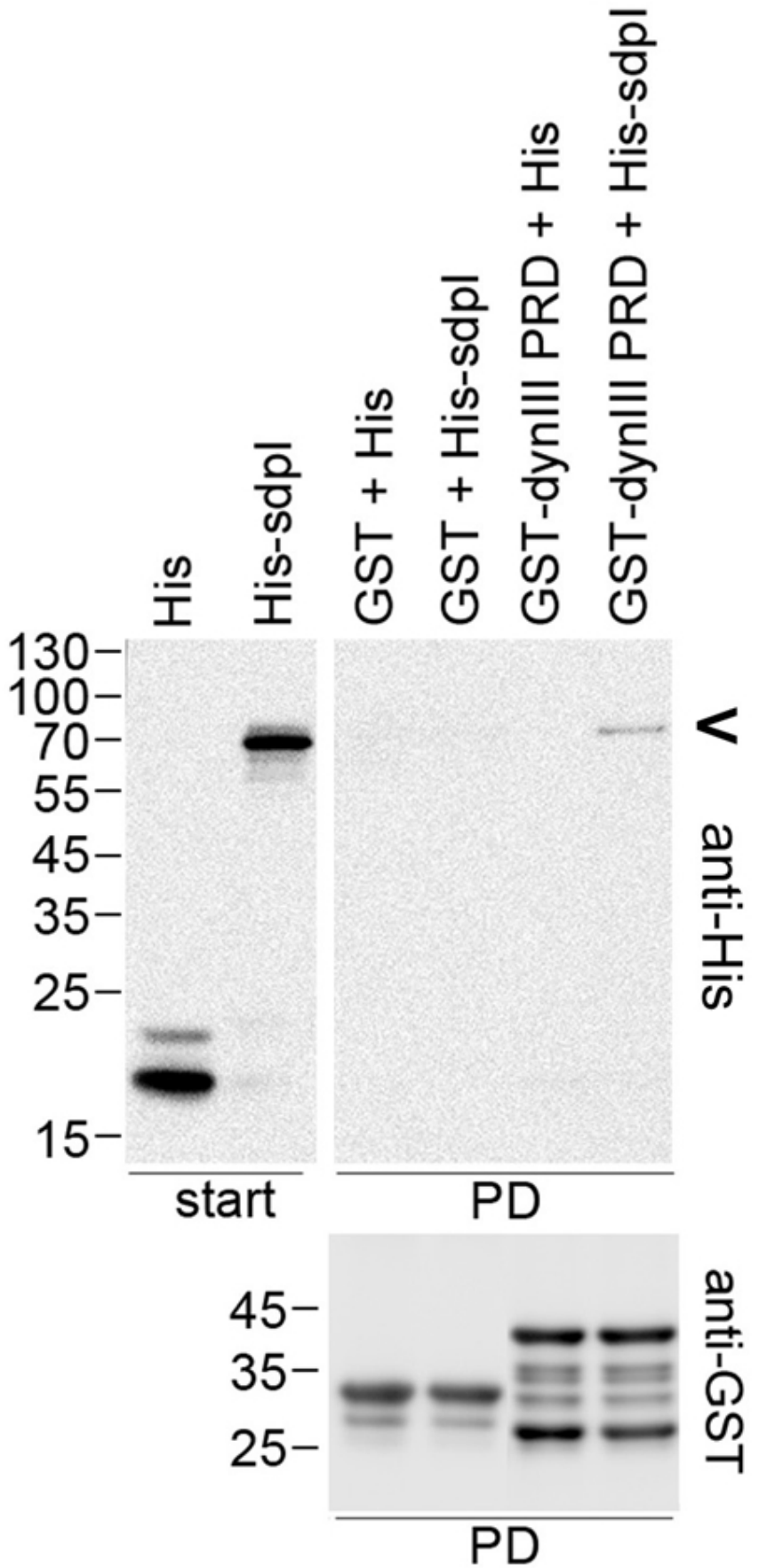

Supplementary Figure 8

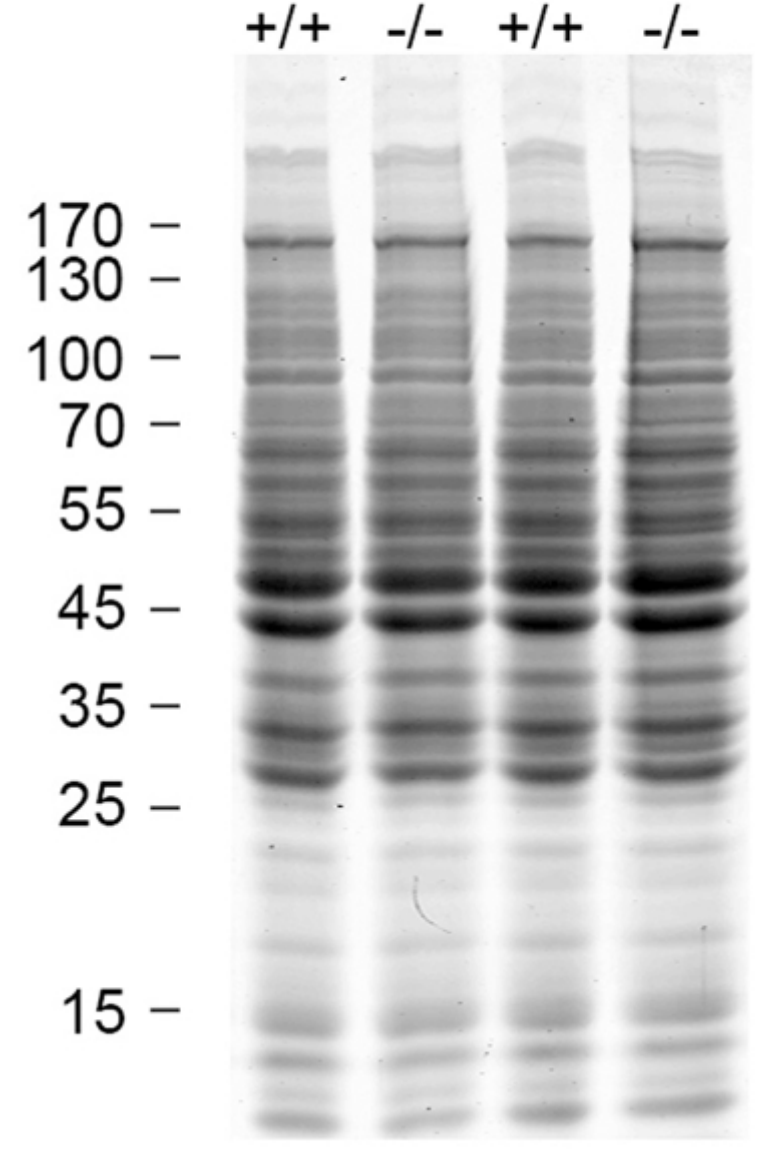

Supplementary Figure 9

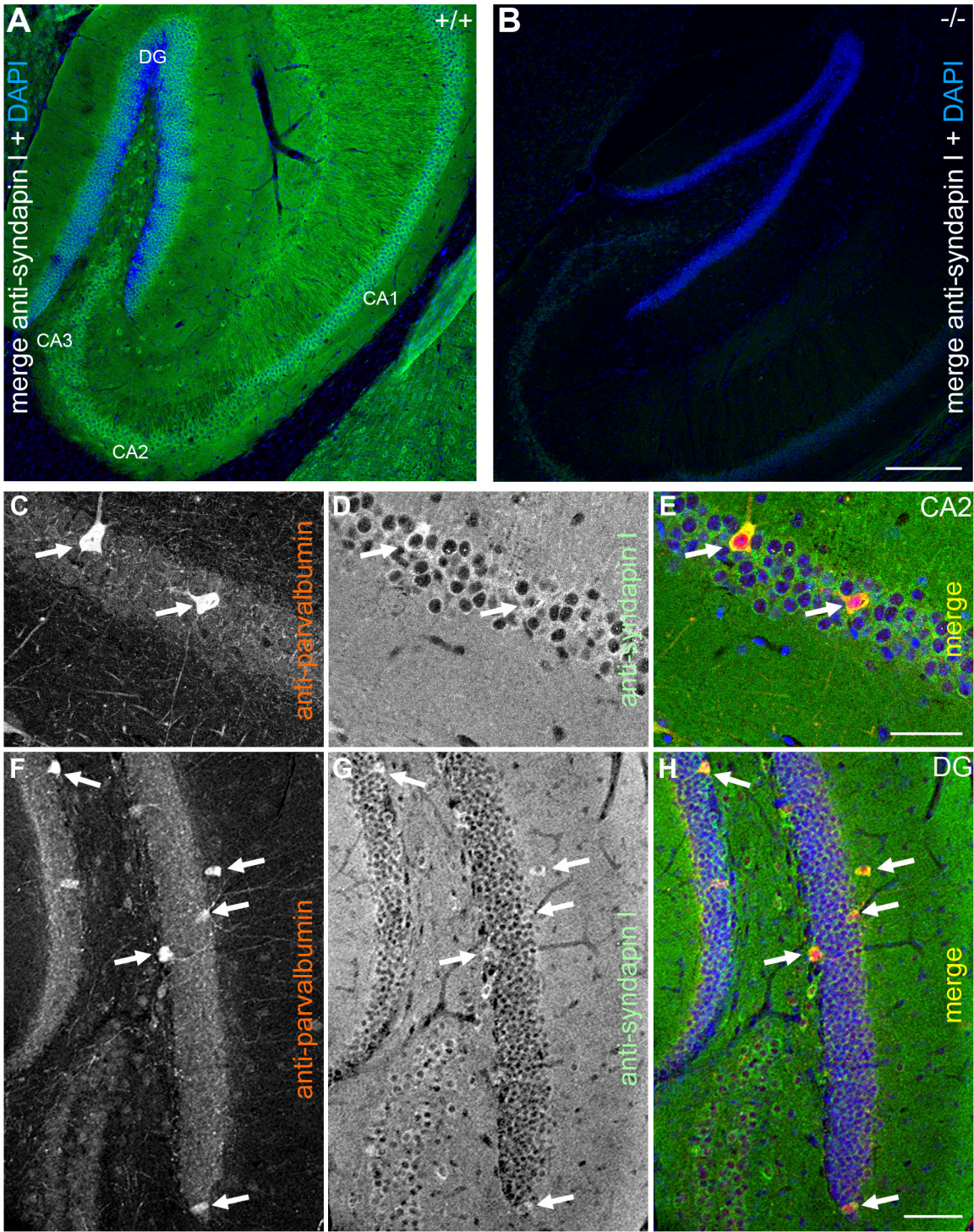

Supplementary Figure 10

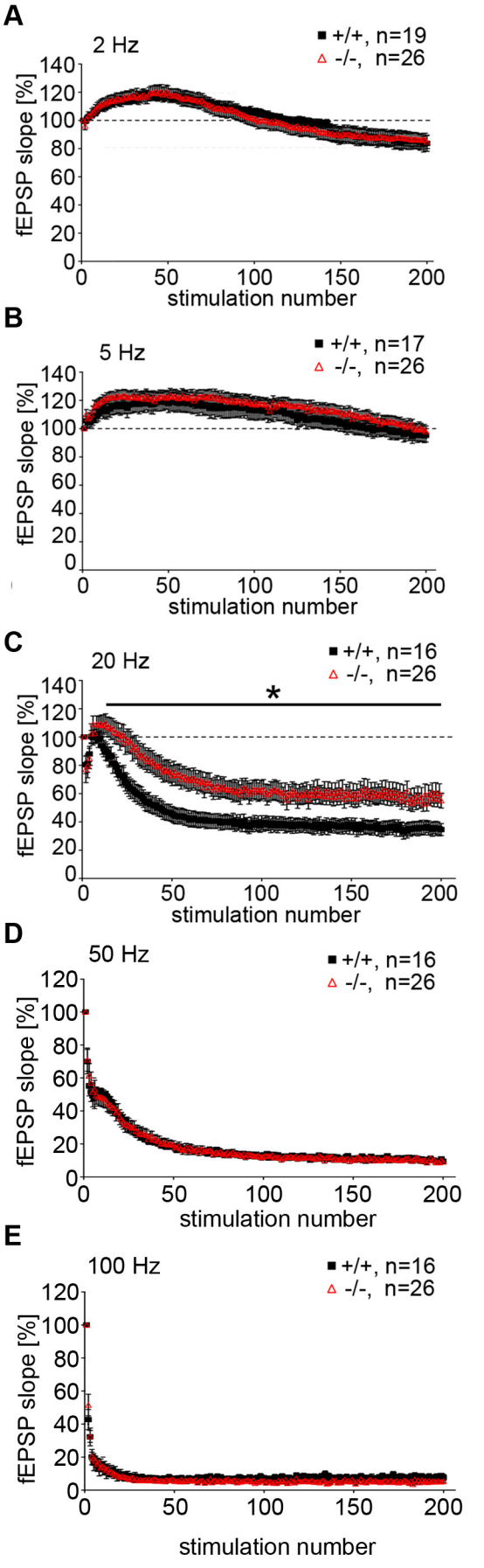

Supplementary Figure 11